Research Square

Preprints are preliminary reports that have not undergone peer review.
They should not be considered conclusive, used to inform clinical practice,
or referenced by the media as validated information.

Macrophage–Tip EC Crosstalk in Proliferative Diabetic Retinopathy: An HLA-DRA/RNF130–TP53INP1 Axis

kunmao ke

kkmsmu@163.com

Jinan University First Affiliated Hospital Department of Ophthalmology https://orcid.org/0000-0003-4935-0135

Research Article

Keywords:

Posted Date: August 31st, 2026

DOI: https://doi.org/10.21203/rs.3.rs-10854453/v1

License: This work is licensed under a Creative Commons Attribution 4.0 International License.
Read Full License

Additional Declarations: The authors declare no competing interests.

Macrophage–Tip EC Crosstalk in Proliferative Diabetic Retinopathy: An HLA-DRA/RNF130–TP53INP1 Axis

Kunmao Ke[1,2*], Qing Zhou[1], Jingxian Zhong[2]

1 Department of Ophthalmology, the First Affiliated Hospital, Jinan University, Guangzhou, China.

2 Department of Ophthalmology, Jiangmen Xinhui Aier New Hope Eye Hospital, Jiangmen, China.

* Correspondence: kkmsmu@163.com; Department of Ophthalmology,the First Affiliated Hospital, Jinan University,613, West Huangpu Avenue, Tianhe District,Guangzhou, Guangdong Province, 510000, China

Abstract

Purpose: To identify causal genes and construct a testable mechanistic hypothesis for macrophage–tip endothelial cell (Tip EC) crosstalk in proliferative diabetic retinopathy (PDR), and to nominate multi-target therapeutic candidates.

Methods: We integrated bulk transcriptomic differential expression, Mendelian randomization with Bayesian colocalization, single-cell RNA sequencing, virtual gene perturbation, and ligand–receptor analysis. Causal genes were validated in an independent dataset. CellChat was used to infer macrophage-to-Tip EC signaling. An AI model and molecular docking were employed for drug repurposing.

Results: Six causal genes were identified; HLA-DRA, RNF130, and TP53INP1 were consistently upregulated in validation. Single-cell analysis localized HLA-DRA/RNF130 to macrophages and TP53INP1 to Tip ECs. Virtual perturbation suggested that HLA-DRA and RNF130 maintain macrophage identity, whereas TP53INP1 regulates extracellular matrix (ECM) remodeling in Tip ECs. CellChat revealed a prominent macrophage–Tip EC communication network dominated by NAMPT–INSR/ITGA5_ITGB1, VEGFA–VEGFR, SPP1–integrin, and TGF-β pathways. Oracillin was identified as a potential multi-target ligand with favorable docking scores to HLA-DRA, RNF130, and TP53INP1.

Conclusions: We propose an HLA-DRA/RNF130–TP53INP1 axis through which macrophages instruct Tip EC matrix remodeling via NAMPT, VEGF, SPP1, and TGF-β pathways in PDR. Oracillin emerges as a multi-target starting point for preclinical validation. This study provides a directly testable model for coupled angiogenesis and fibrosis in diabetic retinopathy.

Introduction

Diabetic retinopathy (DR) is a leading cause of vision loss in working-age adults, with proliferative diabetic retinopathy (PDR) accounting for the majority of severe visual impairment[1,2]. The pathological hallmark of PDR is ischemia-driven retinal neovascularization accompanied by fibrovascular membrane formation, which can cause vitreous hemorrhage and tractional retinal detachment[3]. Intravitreal anti-vascular endothelial growth factor (VEGF) agents are first-line therapy, but incomplete responses, injection burden, and the potential for paradoxical fibrosis highlight the insufficiency of targeting angiogenesis alone[4,5]. There is an urgent need to elucidate the immune–stromal interactions that simultaneously drive both pathological vessel growth and matrix deposition.

Single-cell RNA sequencing (scRNA-seq) has begun to decode the cellular heterogeneity of PDR fibrovascular membranes, identifying macrophages, endothelial cells (ECs), fibroblasts, and other cell types[6]. At the neovascular front, tip endothelial cells (Tip ECs) direct filopodial extension and migration[7], while macrophages—one of the most abundant immune populations in the microenvironment—secrete a repertoire of pro-angiogenic and pro-fibrotic factors[8]. However, the systematic ligand–receptor communication map between macrophages and Tip ECs and the downstream transcriptional programs it controls remain largely undefined.

Furthermore, differential expression analysis alone cannot distinguish causal drivers from secondary changes. Mendelian randomization (MR) with Bayesian colocalization leverages genetic variants to infer causal effects and pinpoint shared causal variants, offering a robust framework for target nomination[9,10]. When combined with single-cell-resolution functional simulation and AI-driven drug repurposing, such an integrative approach holds promise for discovering mechanistic axes that are directly testable in preclinical models.

In this study, we aimed not merely to list candidate genes, but to construct a mechanistic hypothesis for macrophage–Tip EC crosstalk in PDR. By integrating bulk transcriptomics, MR-colocalization, single-cell virtual perturbation, and ligand–receptor analysis, we propose an HLA-DRA/RNF130–TP53INP1 axis that links macrophage immune activation to Tip EC matrix remodeling. We further identify Oracillin as a potential multi-target agent and outline a roadmap for translational validation.

Methods

The overall analytical framework is depicted in Figure 1. All human data were derived from publicly available, ethically approved datasets.

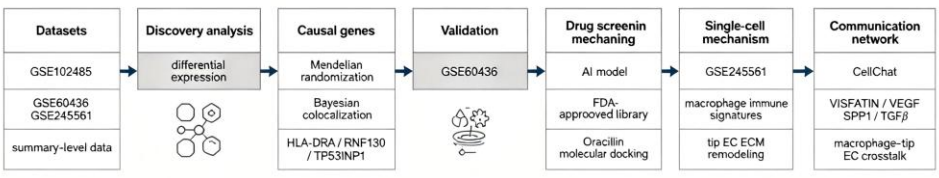


Figure 1. Roadmap of this study.

Bulk Transcriptomic and Causal Gene Identification

The PDR dataset GSE102485 was normalized using RMA, and differentially expressed genes (DEGs) were identified with limma ($|\log2FC| > 1$, adjusted $P < 0.05$)[11,12]. For MR, summary statistics for PDR (1,382 cases, 203,018 controls) were obtained from FinnGen. Instrumental variables were selected from GTEx v8 eQTL data (LD $r^2 < 0.001$, ±1 Mb window)[13]. Inverse-variance weighted (IVW) MR was performed with MR-Egger and weighted median sensitivity analyses using TwoSampleMR[14]. Bayesian colocalization (coloc, PP.H4 > 0.8) was applied to MR-significant DEGs[10]. Intersection of DEGs, MR-significant, and colocalized genes defined the causal gene set.

Validation and Expression Analysis

Expression levels of causal genes were examined in the independent dataset GSE60436. Group differences were assessed by Wilcoxon rank-sum test.

AI Drug Prediction and Molecular Docking

The DrugReflector model[15] was used to predict drugs targeting retinal neovascular membranes in both GSE102485 and GSE60436 (top 500 each). Intersection was taken, and FDA-approved drugs were retained from PubChem. Binding of the selected candidate to HLA-DRA, RNF130, and TP53INP1 was evaluated using CB-Dock2, with a Vina score threshold of –5.0 kcal/mol[16].

Single-Cell RNA-seq Analysis

The PDR fibrovascular membrane scRNA-seq dataset GSE245561 (4 samples) was processed with Seurat (v5.5.0)[17]. After quality filtering (200–6000 genes, <20% mitochondrial reads), data were normalized, integrated with Harmony[18], and clustered using Louvain algorithm (dims = 1:30, resolution = 0.5). UMAP was used for visualization. Cell types were annotated based on canonical markers[6]. Endothelial cells were subtyped into tip (Tip EC), stalk, mature, and immature ECs. Dot plots displayed target gene expression across cell types.

Virtual Gene Perturbation

Virtual knockout and overexpression of HLA-DRA and RNF130 were performed in macrophages, and of TP53INP1 in Tip ECs, using scTenifoldKnk[19]. Significantly responsive genes ($P < 0.05$) were subjected to GO and KEGG enrichment analysis. To focus on consistent biological signals, only pathways emerging from both perturbation directions are reported.

Ligand–Receptor Analysis

CellChat (v1.6.1) was applied to infer communication from macrophages to Tip ECs using the default ligand–receptor database[20]. Significant interactions were defined by

permutation test $P < 0.05$.

Statistical Analysis

All analyses were conducted in R (v4.5.3). Multiple testing was corrected using the Benjamini-Hochberg method.

Results

1. Transcriptomic Data Analysis and Validation

Analysis of the GEO dataset GSE102485 was performed, with normalized box plots shown in Figure 2A. Differential expression analysis yielded a total of 3246 upregulated genes and 1126 downregulated genes (Figure 2B). These differentially expressed genes were subsequently subjected to Mendelian randomization and colocalization analysis to assess their causal relationships (Figure 2C, 2D), ultimately identifying 5 upregulated genes (HLA-DRA, THEMIS, RNF130, TP53INP1, ITGB7) and 1 downregulated gene (MAGI3). The forest plots for these six genes are shown in Figure 2E.

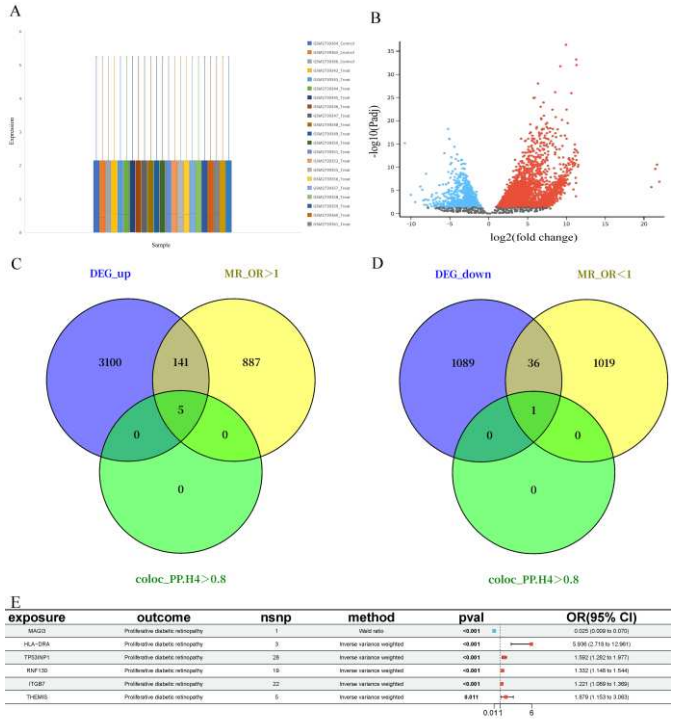


Figure 2. A: Normalized box plot of GSE102485; B: Volcano plot of DEGs in GSE102485; C: Venn diagram of upregulated genes with MR analysis and Bayesian colocalization; D: Venn diagram of downregulated genes with MR analysis and Bayesian colocalization; E: Forest plot of MR analysis results for the six genes.

2. Intergroup Difference Validation

Independent dataset GSE60436 was downloaded for validation analysis. THEMIS was not detected in GSE60436 and could not be validated. Among the remaining

upregulated genes, HLA-DRA, RNF130, and TP53INP1 showed statistically significant differences between the disease and control groups, with the direction of change consistent with the GSE102485 and MR results (Figure 3).

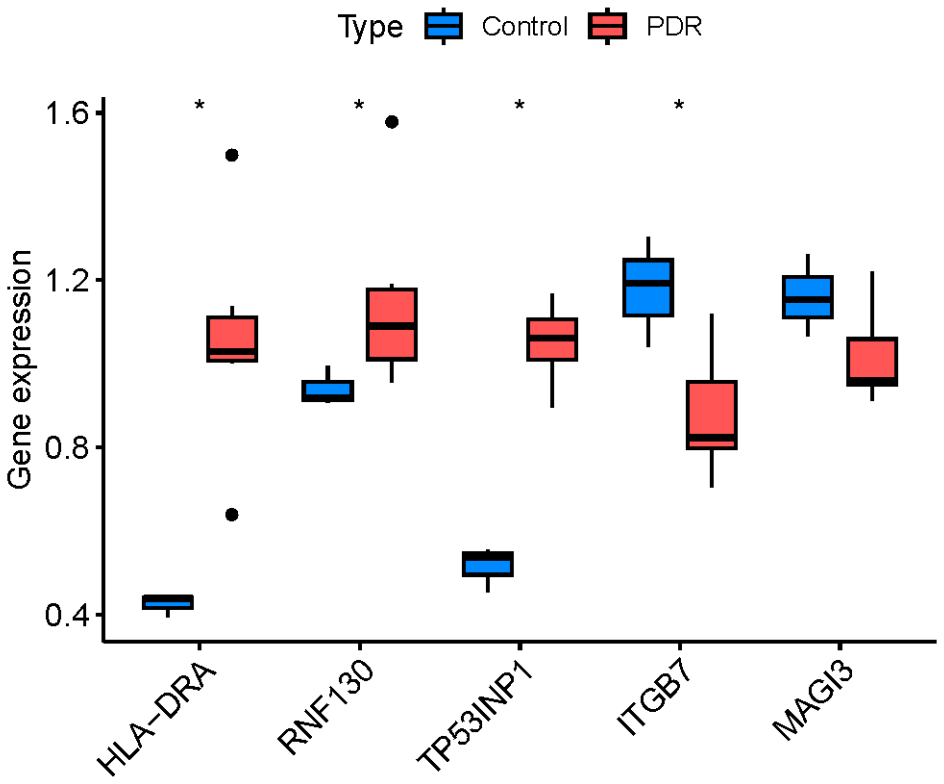


Figure 3. Box plots of the expression of five genes in GSE60436; * $P < 0.05$.

3. AI Drug Prediction and Molecular Docking Validation

Using the DrugReflector model, 500 drugs potentially targeting retinal neovascular membranes were predicted in each of the GSE60436 and GSE102485 datasets. To enhance reliability and reproducibility, the intersection of the two prediction results was taken, yielding a total of 121 drugs (Figure 4A). To accelerate future drug translation, these 121 drugs were sequentially searched in the PubChem database, retaining those approved by the FDA. Ultimately, 40 drugs were obtained, including Bexarotene, Oracillin, dienestrol, etc. (Figure 4B). Because the drug label explicitly warns that Bexarotene can cause fetal malformations, Oracillin, ranked second, was selected for subsequent molecular docking validation based on safety considerations (Figure 4C, 4D, 4E). Molecular docking results showed that the Vina scores of Oracillin with HLA-DRA, RNF130, and TP53INP1 were -7.3, -6.8, and -5.2, respectively, all below the -5.0 kcal/mol threshold. This indicates that Oracillin possesses favorable binding affinity towards these targets, preliminarily verifying its feasibility as a potential therapeutic agent. Among them, the binding energy with HLA-DRA was the lowest, suggesting the most stable interaction, which may be closely related to its immunomodulatory function. Although the binding score for TP53INP1 was relatively lower, it was still within the effective binding range,

implying a possible multi-target synergistic mechanism. These results provide an important theoretical basis and data support for future in-depth exploration of the pharmacological mechanisms and in vivo pharmacodynamic evaluation of Oracillin in neovascular diseases.

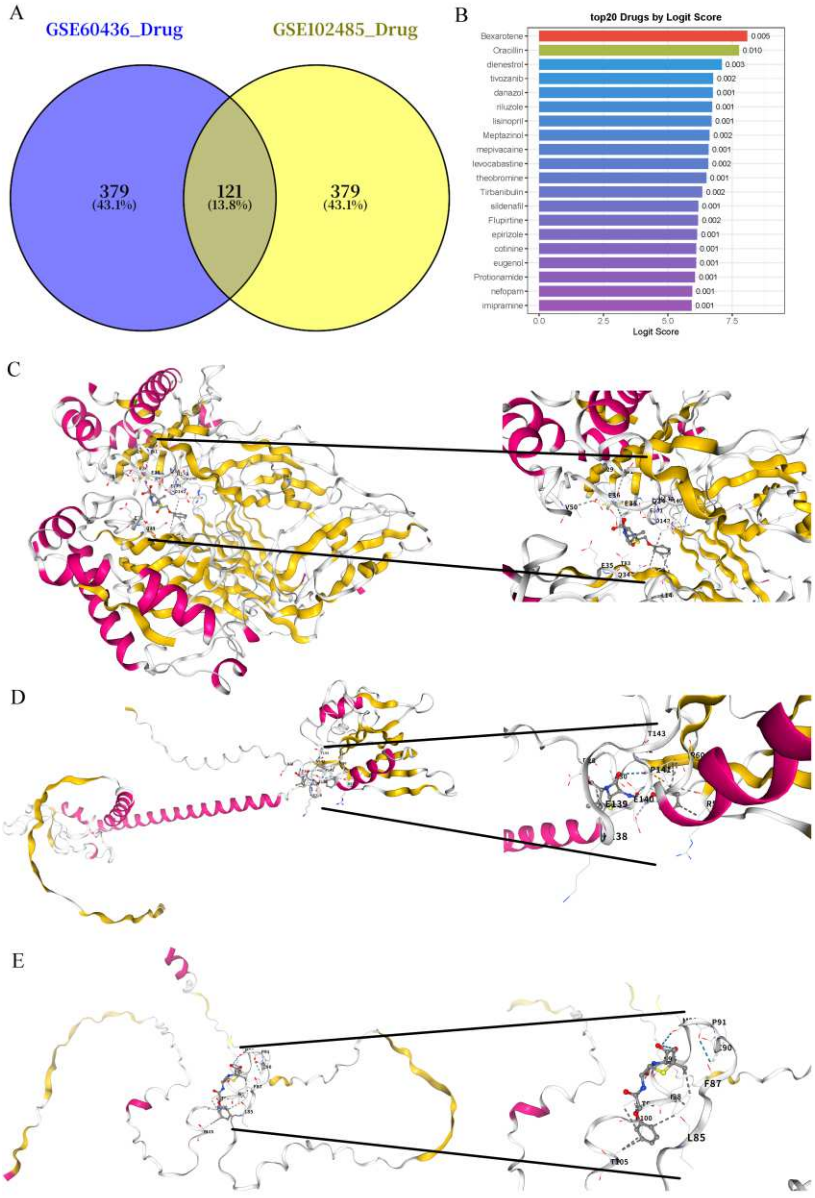


Figure 4. A: Venn diagram of AI drug prediction results; B: Bar chart of FDA-approved drugs; C: Schematic diagram of Oracillin docking with HLA-DRA; D: Schematic diagram of Oracillin docking with RNF130; E: Schematic diagram of Oracillin docking with TP53INP1.

4. Single-Cell Omics Analysis

Single-Cell Landscape and Target Localization

After quality control and integration, 22 cell clusters were identified and annotated into major lineages (Figure 5A–D). ECs were further resolved into tip cells (Tip EC)

responsible for initiating angiogenesis, stalk cells (Stalk EC) responsible for the proliferation and elongation of new vascular sprouts, mature endothelial cells (Mature EC) performing specialized functions, and immature endothelial cells (Immature EC). Dot plot analysis revealed that HLA-DRA and RNF130 were predominantly expressed in macrophages, while TP53INP1 was enriched in Tip ECs (Figure 5E). This cell-type-specific pattern supported their potential functional roles in immune and vascular compartments, respectively.

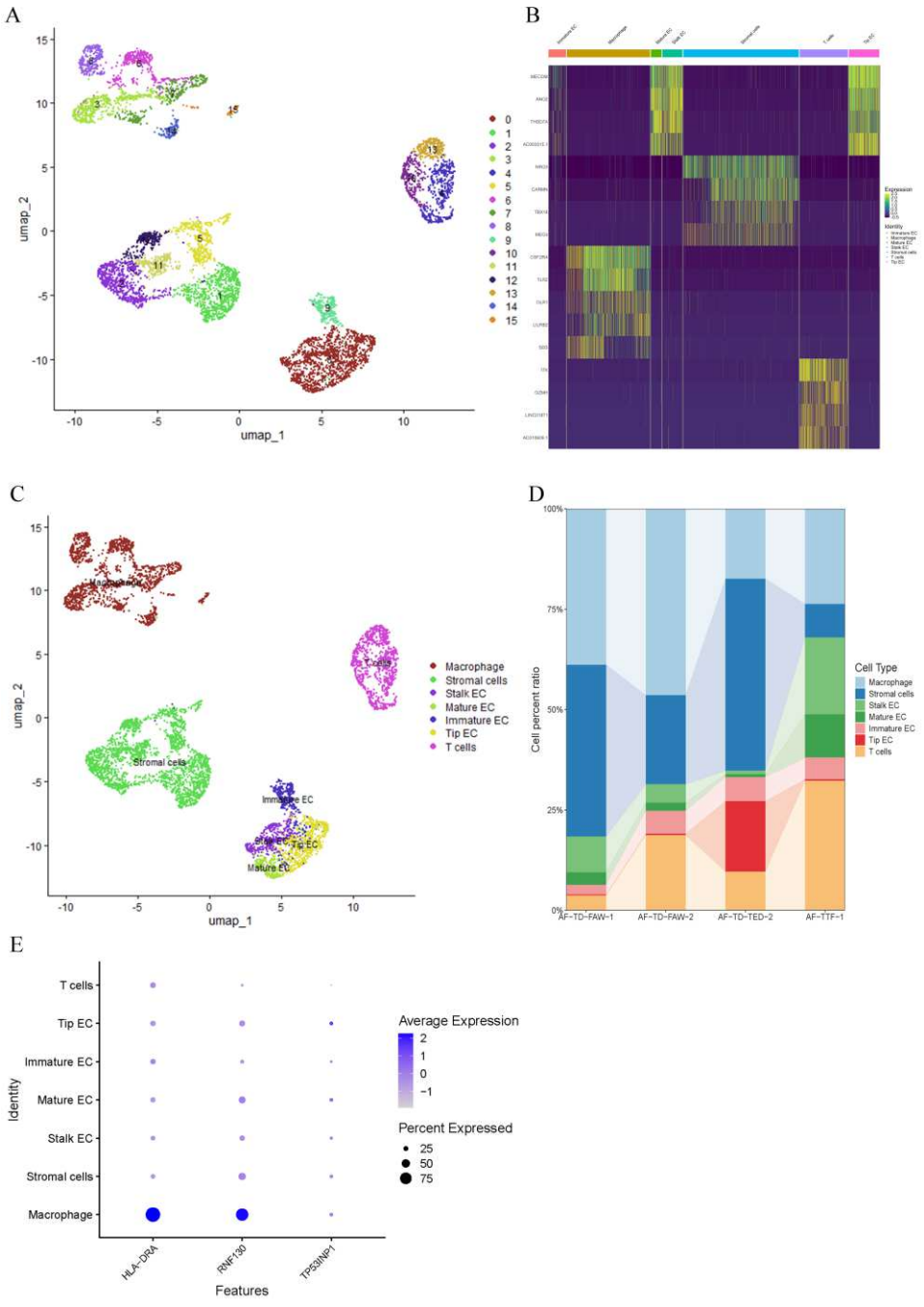


Figure 5. A: UMAP visualization; B: Expression patterns of top 5 marker genes per subpopulation; C: UMAP plot showing the spatial distribution of cell types; D:

Relative abundance of cell populations across samples; E: Expression of HLA-DRA, RNF130, and TP53INP1 across different cell types..

5. Integrated Single-Cell Virtual Perturbation Analysis of HLA-DRA, RNF130, and TP53INP1 in Macrophages and Tip Endothelial Cells

Based on the single-cell dataset GSE245561, both virtual gene knockout and virtual overexpression analyses were performed on identified macrophage and tip endothelial cell clusters to investigate the transcriptional impact of perturbing HLA-DRA, RNF130, and TP53INP1. It should be noted that virtual perturbation (knockout or overexpression) only reflects the degree of change (fold change, FC) in the expression levels of other genes and does not independently indicate the direction of upregulation or downregulation.

HLA-DRA and RNF130 in Macrophages

Virtual knockout of HLA-DRA in macrophages resulted in profoundly altered expression of MS4A1 (FC = 3671.81), RNASE1 (FC = 95.53), RIPOR2 (FC = 62.58), CD79B (FC = 58.25), and AC119396.1 (FC = 43.10) (all $P < 0.001$) (Figure 6A). GO and KEGG enrichment analyses revealed significant involvement in B cell receptor signaling (Figure 6B), B cell differentiation, antigen receptor-mediated signaling, B cell activation, lymphocyte proliferation, immunoglobulin complex, MHC class II protein complex binding, and hematopoietic cell lineage. Similarly, RNF130 knockout (Figure 6C)induced extreme changes in MS4A1 (FC = 3896.92), RNASE1 (FC = 92.61), CD52 (FC = 19.60), and RIPOR2 (FC = 17.17) ($P < 0.05$), with enrichment in lymphocyte proliferation and MHC class II/immunoglobulin binding, and KEGG enrichment solely in hematopoietic cell lineage (Figure 6D). Both knockouts thus drove massive fold changes in B cell markers and activated B cell lineage programs, suggesting that HLA-DRA and RNF130 are critical for maintaining the intrinsic transcriptional identity of macrophages.

In contrast, virtual overexpression of HLA-DRA prominently altered S100A11 (FC = 51.10), C1QA (FC = 42.42), C1QC (FC = 23.92), CD14 (FC = 23.86), and C1QB (FC = 18.87) (all with strong significance), with enrichments in complement activation (classical pathway), humoral immune response mediated by circulating immunoglobulin, synapse pruning, IgG/immunoglobulin binding, and complement and coagulation cascades (Figure 7A). Overexpression of RNF130 yielded an even stronger signature, including S100A11 (FC = 323.54), C1QB (FC = 226.10), TMEM176B (FC = 176.64), C1QA (FC = 148.04), C1QC (FC = 145.98), as well as LGALS1, ACTB, TREM2, and APOE (Figure 7C). Functional enrichment again highlighted complement activation, humoral immune response, immunoglobulin/IgG binding, and amyloid-beta binding, with the complement and coagulation cascades as the primary KEGG pathway (Figure 7B, 7D). Thus, overexpression of HLA-DRA and RNF130 synergistically enhanced complement-related immunomodulatory functions in macrophages.

TP53INP1 in Tip Endothelial Cells

Virtual knockout of TP53INP1 (Figure 6E) in tip cells significantly altered

IGFBP2 (FC = 245.96), NTRK3 (FC = 165.60), STK32B (FC = 128.92), COLEC12 (FC = 106.72), and LINC01748 (FC = 95.63) (all $P < 0.001$), along with multiple extracellular matrix (ECM) and vascular remodeling genes such as COL12A1, COL5A1, LOX, PDGFB, and WNT5A. Enrichment analysis (Figure 6F) demonstrated involvement in fibroblast growth factor receptor signaling, connective tissue development, ECM organization, collagen trimers, ECM structural constituents, growth factor binding, cell adhesion mediator activity, and the Ras signaling pathway. Virtual overexpression of TP53INP1 (Figure 7E) produced massive changes, with top genes including GJA5 (FC = 1157.75), SULT1B1 (FC = 311.39), STK32B (FC = 97.32), GPRIN3 (FC = 89.65), and PGF (FC = 76.46), again accompanied by ECM and angiogenic genes such as COLEC12, NTRK3, LOX, COL5A1, and WNT5A. Enriched terms (Figure 7F) included excitatory synapse assembly, cell chemotaxis, regulation of protein phosphorylation and synaptic plasticity, ECM/collagen trimer, ECM structural constituents, cell adhesion mediator activity, Ras signaling, and protein digestion and absorption. Both loss- and gain-of-function perturbations broadly affected gene programs related to ECM remodeling, cell adhesion, and growth factor signaling, indicating that TP53INP1 serves as a key regulatory node balancing the matrix remodeling functions of tip endothelial cells.

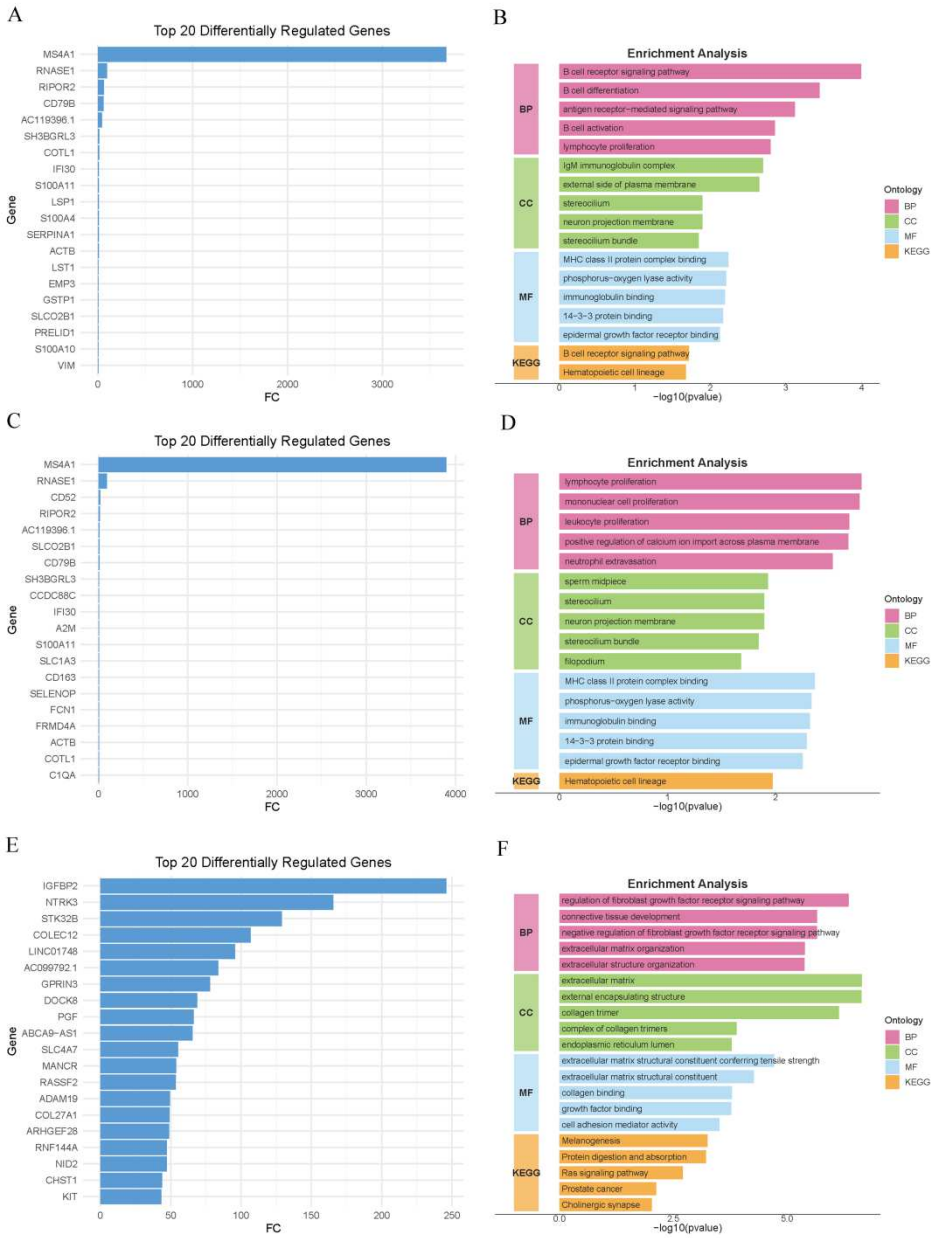


Figure 6. A: Gene expression changes after virtual knockout of HLA-DRA in macrophages; B: GO and KEGG analysis of changed genes after virtual HLA-DRA knockout in macrophages; C: Gene expression changes after virtual knockout of RNF130 in macrophages; D: GO and KEGG analysis of changed genes after virtual RNF130 knockout in macrophages; E: Gene expression changes after virtual knockout of TP53INP1 in Tip ECs; F: GO and KEGG analysis of changed genes after virtual TP53INP1 knockout in Tip ECs.



Figure 7. A: Gene expression changes after virtual overexpression of HLA-DRA in macrophages; B: GO and KEGG analysis of changed genes after virtual HLA-DRA overexpression in macrophages; C: Gene expression changes after virtual overexpression of RNF130 in macrophages; D: GO and KEGG analysis of changed genes after virtual RNF130 overexpression in macrophages; E: Gene expression changes after virtual overexpression of TP53INP1 in Tip ECs; F: GO and KEGG analysis of changed genes after virtual TP53INP1 overexpression in Tip ECs.

7. Macrophage–Tip EC Communication Network

CellChat identified 23 significant ligand–receptor pairs from macrophages to Tip ECs (Table 1, Figure 8). The NAMPT (visfatin) pathway dominated: NAMPT–INSR

(prob = 0.314) and NAMPT–ITGA5_ITGB1 (prob = 0.139) were the top interactions. VEGF pathways (VEGFA/B–VEGFR1/2) and SPP1–multiple integrins (ITGAV_ITGB1, ITGA5_ITGB1, etc.) were prominently active. TGF-β1 signaling via TGFβR and ACVR1 complexes, as well as IGF1–IGF1R and CXCL12–CXCR4 axes, further contributed. Cell–cell contact signals included PECAM1 and ITGB2–ICAM2. These data reveal a multimodal network through which macrophages simultaneously deliver pro-angiogenic, pro-migratory, and pro-fibrotic cues to Tip ECs, with NAMPT serving as a potential master coordinator.

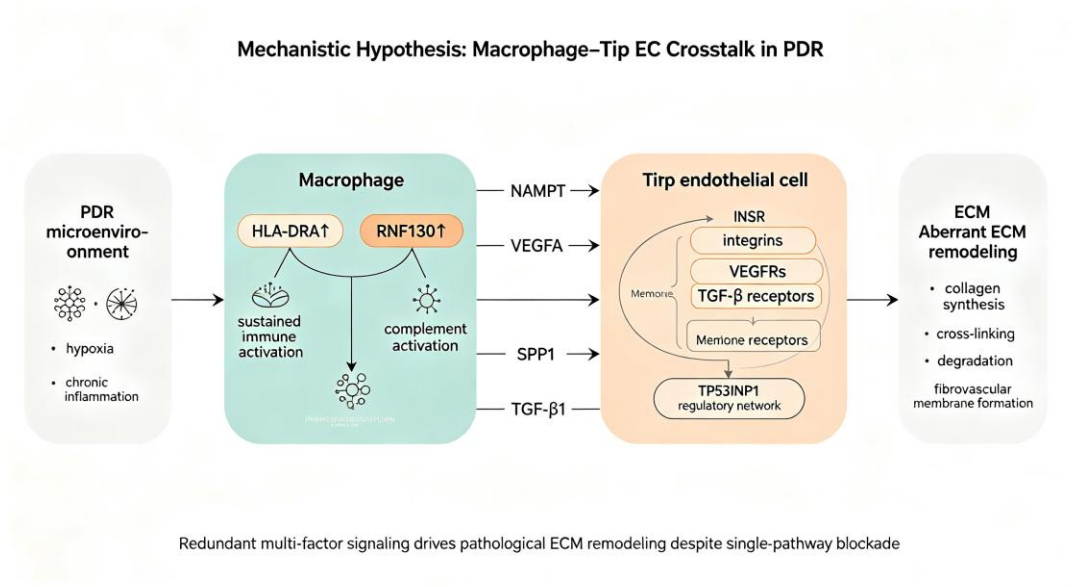


Figure 8 synthesizes these findings into a working model of the HLA-DRA/RNF130–TP53INP1 axis.

Table 1. Results of ligand-receptor communication analysis between macrophages and tip endothelial cells.

source	target	ligand	receptor	prob	pval
Macrophage	Tip EC	TGFB1	TGFbR1_R2	0.011278	0
Macrophage	Tip EC	TGFB1	ACVR1_TGFbR	0.012087	0
Macrophage	Tip EC	VEGFA	FLT1	0.022882	0
Macrophage	Tip EC	VEGFA	KDR	0.013903	0
Macrophage	Tip EC	VEGFB	FLT1	0.040104	0
Macrophage	Tip EC	VEGFA	FLT1_KDR	0.021464	0
Macrophage	Tip EC	IGF1	IGF1R	0.001231	0
Macrophage	Tip EC	CXCL12	CXCR4	0.004525	0
Macrophage	Tip EC	CXCL12	ACKR3	0.005016	0
Macrophage	Tip EC	MIF	ACKR3	0.038464	0
Macrophage	Tip EC	SPP1	ITGAV_ITGB1	0.007568	0
Macrophage	Tip EC	SPP1	ITGA9_ITGB1	0.007983	0
Macrophage	Tip EC	SPP1	ITGA5_ITGB1	0.015263	0
Macrophage	Tip EC	NAMPT	INSR	0.314373	0

Macrophage	Tip EC	NAMPT	ITGA5_ITGB1	0.138935	0
Macrophage	Tip EC	GRN	SORT1	0.009802	0
Macrophage	Tip EC	COL1A1	ITGA2_ITGB1	0.003847	0
Macrophage	Tip EC	COL1A2	ITGA2_ITGB1	0.00456	0
Macrophage	Tip EC	FN1	ITGA5_ITGB1	0.012121	0.01
Macrophage	Tip EC	COL1A1	ITGA9_ITGB1	0.003348	0
Macrophage	Tip EC	COL1A2	ITGA9_ITGB1	0.003968	0
Macrophage	Tip EC	COL1A1	ITGA10_ITGB1	0.002517	0
Macrophage	Tip EC	COL1A2	ITGA10_ITGB1	0.002984	0
Macrophage	Tip EC	ADGRE5	CD55	0.001048	0
Macrophage	Tip EC	ITGB2	ICAM2	0.009382	0
Macrophage	Tip EC	PECAM1	PECAM1	0.042067	0

Discussion

By integrating causal inference with single-cell functional prediction, this study constructs a novel mechanistic model of PDR fibrovascular membrane formation. We propose that macrophages, governed by HLA-DRA and RNF130, secrete a cocktail of paracrine signals—dominated by NAMPT—that instruct Tip ECs to execute matrix remodeling via TP53INP1. This immune–vascular axis provides a conceptual framework for the coupled pathology of angiogenesis and fibrosis that limits current anti-VEGF therapy[21].

HLA-DRA/RNF130 as Gatekeepers of Macrophage Identity

Our virtual perturbation results reveal a striking functional duality. Knockdown of HLA-DRA or RNF130 in macrophages derepressed B-cell lineage programs, implying that these molecules are essential for maintaining macrophage transcriptional identity. HLA-DRA encodes the alpha chain of MHC class II and is known to regulate M1 polarization and NF-κB signaling[22]. RNF130 is an E3 ubiquitin ligase implicated in immune regulation and pulmonary fibrosis[23]. Their convergent effect on lineage fidelity raises the hypothesis that RNF130 may modulate MHC class II machinery via ubiquitination. Conversely, overexpression of either gene amplified complement C1q expression. Given that complement activation is documented in PDR vitreous[24] and has been shown to exacerbate retinal inflammation and vascular damage in diabetic retinopathy[25], sustained upregulation of HLA-DRA/RNF130 in the diabetic milieu may paradoxically amplify local inflammatory cascades, tipping macrophages toward a hyper-reactive state.

TP53INP1: A Matrix Rheostat in Tip Endothelial Cells

TP53INP1 is traditionally viewed as a p53 target involved in autophagy and stress response[26]. However, emerging evidence has linked TP53INP1 to endothelial cell function: hypoxic mesenchymal stem cell-derived exosomal miR-125b was shown to promote endothelial cell survival and migration by directly targeting

TP53INP1[27]. Our data reposition it as a key modulator of ECM organization in Tip ECs. Both loss- and gain-of-function perturbations consistently affected collagens, LOX, and growth factor signaling. This suggests that TP53INP1 serves as a "matrix rheostat" whose dysregulation by incoming macrophage-derived signals (e.g., TGF-β1, NAMPT) leads to pathological ECM accumulation at the neovascular front—a hallmark of fibrovascular membranes.

The NAMPT Axis Bridges Inflammation and Fibrosis

The most prominent communication channel we identified is the NAMPT–INSR/ITGA5_ITGB1 interaction. Extracellular NAMPT (visfatin) is a pleiotropic adipocytokine with pro-angiogenic, pro-inflammatory, and ECM-modulating activities[28,29]. Critically, NAMPT levels are elevated in the vitreous of patients with proliferative diabetic retinopathy[30], and visfatin has been demonstrated to directly stimulate retinal endothelial cell proliferation, migration, and tube formation[30], as well as the production of VEGF and matrix metalloproteinases[31]. Its simultaneous engagement of INSR (a metabolic receptor) and the classic fibronectin receptor ITGA5_ITGB1 provides a mechanistic basis for the coordinated activation of metabolic, adhesive, and migratory programs in Tip ECs. This may explain why angiogenesis and fibrosis are so tightly linked in PDR and why anti-VEGF alone fails to halt matrix deposition. Indeed, anti-VEGF monotherapy has been reported to paradoxically shift the angiogenic balance toward fibrosis in some PDR patients[21]. The NAMPT–integrin axis could therefore represent a parallel, VEGF-independent pathway sustaining pathological remodeling.

Oracillin as a Multi-Target Starting Point

Our AI pipeline identified Oracillin, an FDA-approved antibiotic, as a potential multi-target ligand for HLA-DRA, RNF130, and TP53INP1. While its conventional indication is unrelated, the β-lactam scaffold may possess unrecognized immunomodulatory properties. Certain β-lactam antibiotics have been shown to modulate neutrophil function and inflammatory cytokine release through direct interactions with host cell targets[32]. The strongest docking to HLA-DRA hints that its primary mode could be stabilization of MHC class II function, thereby tempering macrophage hyperactivation and downstream matrix signaling. However, these are entirely computational predictions. Future surface plasmon resonance and cell-based assays are obligatory to confirm binding and functional effects. Importantly, local intravitreal delivery could circumvent systemic antimicrobial concerns and drug resistance issues.

Limitations and Future Directions

This study is hypothesis-generating and relies on in silico analyses. All virtual perturbations require validation through CRISPR-Cas9 editing or pharmacological inhibition in primary macrophages and endothelial cells. The single-cell dataset comprises only four membranes; larger cohorts are needed. MR, though robust, cannot fully exclude horizontal pleiotropy, which we mitigated with strict

colocalization. The functional role of RNF130 as a ubiquitin ligase in this context remains speculative, and its substrates in macrophages must be identified.

To bridge computational prediction to clinical translation, we have designed a three-phase validation roadmap: (1) In vitro: knockdown/overexpression of HLA-DRA, RNF130, and TP53INP1 in macrophages and Tip ECs, followed by Transwell co-culture and neutralizing antibodies against NAMPT and SPP1 to confirm crosstalk; (2) In vivo: multiplex immunofluorescence on human PDR membranes to confirm co-localization, and cell-type-specific AAV-mediated gene interference in STZ-induced diabetic oxygen-induced retinopathy (OIR) mice; (3) Therapeutic testing: surface plasmon resonance for Oracillin binding kinetics, intravitreal pharmacokinetics in mice, and efficacy evaluation in the diabetic OIR model. This roadmap directly tests the HLA-DRA/RNF130–TP53INP1 axis and the therapeutic potential of Oracillin.

Conclusion

This integrative multi-omics study proposes a macrophage–Tip EC communication network centered on an HLA-DRA/RNF130–TP53INP1 axis in PDR. We nominate NAMPT as a key molecular bridge and Oracillin as a multi-target candidate for further development. The model offers directly testable hypotheses for the coupled pathogenesis of angiogenesis and fibrosis in diabetic retinopathy and aligns with the translational mission of vision science.

Patents

Author Contributions: Conceptualization, KM.K.; methodology, KM.K.; data analysis and in-terpretation, KM.K.; writing—original draft preparation, KM.K.; writing—review and editing, Q.Z. and JX.Z. All authors have read and agreed to the published version of the manuscript.
Funding: This research received no external funding.
Institutional Review Board Statement: Not applicable. All data used in this study were derived from publicly available GWAS summary datasets, which had received approval from the relevant ethics committees. No human data were collected in this study; therefore, further ethical approval was not necessary.
Informed Consent Statement: Not applicable.
Clinical trial number: not applicable.
Data Availability Statement: FinnGen (https://www.finngen.fi/en; accessed January 1, 2026).
Acknowledgments: The authors have reviewed and edited the output and take full responsibility for the content of this publication.
Conflicts of Interest: The authors declare no conflicts of interest.
Declaration of generative AI and AI-assisted technologies in the manuscript preparation process: During the preparation of this work, the author(s) used DeepSeek for language polishing and refinement. After using this tool, the author(s) have

carefully reviewed and verified all content, and take full responsibility for its accuracy, comprehensiveness, and impartiality.

References:

[1]Yau JW, Rogers SL, Kawasaki R, et al. Global prevalence and major risk factors of diabetic retinopathy. Diabetes Care. 2012;35:556-564.

[2]Cheung N, Mitchell P, Wong TY. Diabetic retinopathy. Lancet. 2010;376:124-136.

[3]Antonetti DA, Klein R, Gardner TW. Diabetic retinopathy. N Engl J Med. 2012;366:1227-1239.

[4]Seo H, Park SJ, Song M. Diabetic Retinopathy: Mechanisms, Current Therapies, and Emerging Strategies. Cells. 2025;14:376.

[5]Klaassen I, Van Noorden CJ, Schlingemann RO. Molecular basis of the inner blood-retinal barrier and its breakdown. Prog Retin Eye Res. 2013;34:19-48.

[6]Corano Scheri K, Lavine JA, Tedeschi T, et al. Single-cell transcriptomics analysis of PDR fibrovascular membranes reveals AEBP1 as fibrogenesis modulator. JCI Insight. 2023;8:e172062.

[7]Zarkada G, Howard JP, Xiao X, et al. Specialized endothelial tip cells guide neuroretina vascularization. Dev Cell. 2021;56:2237-2251.

[8]Zhou H, Zhang L, Ding C, et al. Upregulation of HMOX1 associated with M2 macrophage infiltration in PDR. Int Immunopharmacol. 2024;134:112231.

[9]Davey Smith G, Hemani G. Mendelian randomization. Hum Mol Genet. 2014;23:R89-98.

[10]Giambartolomei C, Vukcevic D, Schadt EE, et al. Bayesian test for colocalisation. PLoS Genet. 2014;10:e1004383.

[11]Ritchie ME, Phipson B, Wu D, et al. limma powers differential expression analyses. Nucleic Acids Res. 2015;43:e47.

[12]Edgar R, Domrachev M, Lash AE. Gene Expression Omnibus. Nucleic Acids Res. 2002;30:207-210.

[13]GTEx Consortium. The GTEx Consortium atlas. Science. 2020;369:1318-1330.

[14]Hemani G, Zheng J, Elsworth B, et al. The MR-Base platform. Elife. 2018;7:e34408.

[15]Ledford H. This AI method could turbocharge the hunt for new medicines. Nature. 2025 Oct 23.

[16]Liu Y, Yang X, Gan J, et al. CB-Dock2. Nucleic Acids Res. 2022;50:W159-W164.

[17]Hao Y, Hao S, Andersen-Nissen E, et al. Integrated analysis of multimodal single-cell data. Cell. 2021;184:3573-3587.

[18]Korsunsky I, Millard N, Fan J, et al. Fast, sensitive and accurate integration with Harmony. Nat Methods. 2019;16:1289-1296.

[19]Osorio D, Zhong Y, Li G, et al. scTenifoldKnk: virtual knockout tool. Patterns. 2022;3:100434.

[20]Jin S, Guerrero-Juarez CF, Zhang L, et al. CellChat for inference of intercellular communication. Nat Commun. 2021;12:1088.

[21]Van Geest RJ, Lesnik-Oberstein SY, Tan HS, et al. A shift in the balance of vascular endothelial growth factor and connective tissue growth factor by bevacizumab causes the angiofibrotic switch in proliferative diabetic retinopathy. Invest Ophthalmol Vis Sci. 2012;53:4646-4654.
[22]Xiong F, Wang B, Zhang H, et al. HLA-DRA promotes M2 to M1 polarization via NF-κB. Int Immunopharmacol. 2025;144:113706.
[23]Zhang J, Chen W, Du J, et al. RNF130 protects against pulmonary fibrosis. Int Immunopharmacol. 2023;117:109985.
[24] Shahulhameed S, Vishwakarma S, Chhablani J, et al. A Systematic Investigation on Complement Pathway Activation in Diabetic Retinopathy. Front Immunol. 2020;11:154.
[25] Pan WW, Lin F, Fort PE. The innate immune system in diabetic retinopathy. Prog Retin Eye Res. 2021;84:100940.
[26]Tomasini R, Seux M, Nowak J, et al. TP53INP1 is a novel p73 target gene. Oncogene. 2005;24:8093-8104.
[27] Zhang XF, Wang T, Wang ZX, et al. Hypoxic ucMSC-secreted exosomal miR-125b promotes endothelial cell survival and migration during wound healing by targeting TP53INP1. Mol Ther Nucleic Acids. 2021;26:347-359.
[28]Semerena E, Nencioni A, Masternak K. Extracellular NAMPT in disease. Front Immunol. 2023;14:1268756.
[29]Dakroub A, Nasser SA, Kobeissy F, et al. Visfatin: an emerging adipocytokine. J Cell Physiol. 2021;236:6282-6296.
[30]Dakroub A, Nasser SA, Kobeissy F, et al. Visfatin: An emerging adipocytokine bridging the gap in the evolution of cardiovascular diseases. J Cell Physiol. 2021;236(9):6282-6296.
[31]Adya R, Tan BK, Chen J, et al. Visfatin induces human endothelial VEGF and MMP-2/9 production via MAPK and PI3K/Akt signalling pathways: novel insights into visfatin-induced angiogenesis. Diabetes Care. 2008;31:758-760.
[32]Oh J, Patel J, Park HB, Crawford JM. β-Lactam Biotransformations Activate Innate Immunity. J Org Chem. 2018;83(13):7173-7179.